ACS chemical biology

pubs.acs.org/acschemicalbiology

Letters

Peptide Probes for *Plasmodium falciparum* MyoA Tail Interacting Protein (MTIP): Exploring the Druggability of the Malaria Parasite Motor Complex

Charlie N. Saunders, Ernesto Cota, Jake Baum, and Edward W. Tate*

Cite This: *ACS Chem. Biol.* 2020, 15, 1313−1320

Read Online

ACCESS | Metrics & More | Article Recommendations | Supporting Information

ABSTRACT: Malaria remains an endemic tropical disease, and the emergence of *Plasmodium falciparum* parasites resistant to current front-line medicines means that new therapeutic targets are required. The *Plasmodium* glideosome is a multiprotein complex thought to be essential for efficient host red blood cell invasion. At its core is a myosin motor, Myosin A (MyoA), which provides most of the force required for parasite invasion. Here, we report the design and development of improved peptide-based probes for the anchor point of MyoA, the *P. falciparum* MyoA tail interacting protein (*Pf*MTIP). These probes combine low nanomolar binding affinity with significantly enhanced cell penetration and demonstrable competitive target engagement with native *Pf*MTIP through a combination of Western blot and chemical proteomics. These results provide new insights into the potential druggability of the MTIP/MyoA interaction and a basis for the future design of inhibitors.

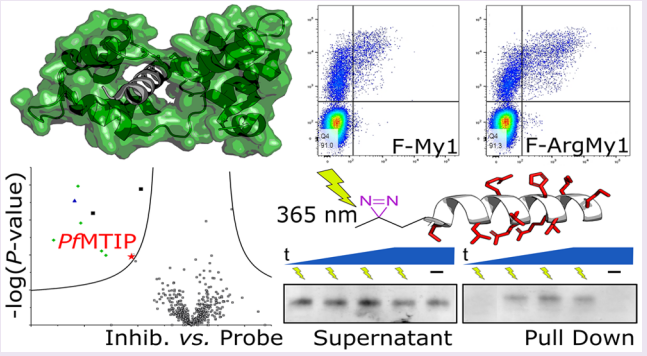

Despite centuries of endeavor, malaria remains an endemic tropical disease infecting hundreds of millions of people each year and leading to hundreds of thousands of deaths. Treatment using artemisinin-based combination therapies (ACTs, the current gold standard therapeutic) alongside extensive deployment of insecticide-treated bed nets has led to a marked reduction in deaths and infections. However, the 2018 WHO malaria report indicated that there had been an increase of 5 million reported infections, to a total of approximately 219 million across the tropics.[1] Additionally, the rise of ACT-resistant parasites has been recorded in multiple countries throughout South East Asia, and more recently in Eastern India.[2,3] While this resistance may not be the direct cause of the increase in infections, it does highlight a need for new therapeutic targets. The *Plasmodium* glideosome complex houses several key protein−protein interactions (PPIs) thought to be required for efficient host cell invasion, an essential step in the parasite lifecycle. One such PPI is the anchor point for Myosin A (MyoA), an actomyosin motor thought to contribute to the force required during an invasion event (Figure 1a).[4] The anchor point for this invasion force is provided by the buried clamp-like interaction between the tail of the parasite's myosin motor myosin A (MyoA) and its light chain, Myosin A tail interacting protein (MTIP; Figure 1b). This interaction has previously been studied *in vitro* using a variety of binding assays, NMR, and an alanine mutation scan, attributing tight binding to key amino acids on each face of the helical MyoA tail.[5,6]

Recent work has demonstrated that the MyoA motor is essential for malaria parasite invasion of the human red blood cell in the most virulent species affecting people, *P. falciparum*, corroborated by studies in a related apicomplexan parasite, *Toxoplasma gondii*.[8,9] *Tg*MyoA-KO parasites showed a rate of invasion almost 20-fold slower compared to *WT* parasites, meaning that although parasites completed the invasion process, the invasion event lasted 10 min rather than 30 s.[8] A truncated *Plasmodium yeolii* MyoA[803−817] peptide was previously claimed to inhibit the growth of a *P. falciparum* culture, with IC_{50} = 84 μM.[10] However, the targets engaged and localization/uptake of the peptide were undetermined, and subsequent work has cast doubt on this conclusion.[6]

While the MyoA:MTIP PPI offers a potentially exciting therapeutic target, it presents a number of challenges, particularly the localization of the fully formed MyoA:MTIP complex *in vivo* behind three unique membranes: the host erythrocyte plasma membrane, the parasitophorous vacuole

Received: April 26, 2020
Accepted: May 8, 2020
Published: May 8, 2020

https://dx.doi.org/10.1021/acschembio.0c00328
ACS Chem. Biol. 2020, 15, 1313−1320

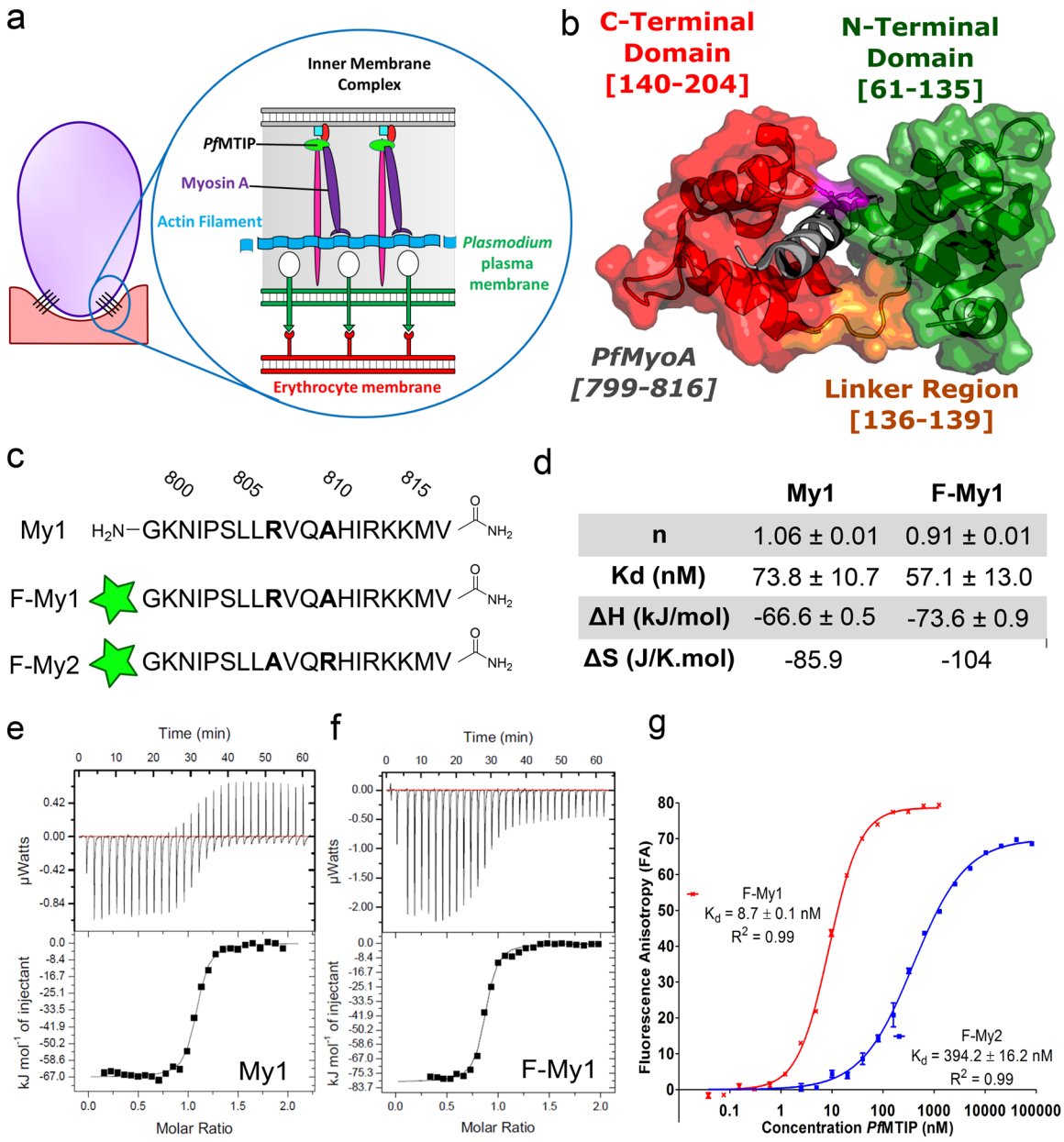

Figure 1. Binding of My1, F-My1, and F-My2 to PfMTIP. (a) Linear model of *P. falciparum* glideosome and motor complex, within the context of erythrocyte host cell invasion. Adapted from Cowman et al.[7] (b) Annotated crystal structure of a truncated Myosin-A peptide [799−816] (gray) clamped by recombinant PfMTIP, highlighting the C- (red) and N-terminal regions (green).[5] (c) Peptide sequences and N-/C-terminal modifications for synthesized peptides based on the truncated PfMyoA[799−816] sequence, with an additional N-terminal glycine spacer. Green star indicates addition of a 5(6)-carboxyfluorescein moiety. (d) Thermodynamic parameters for ITC experiment of binding between My1 and F-My1 peptides and PfMTIP (n = 2). (e) My1 peptide ITC binding isotherm titrated into PfMTIP. (f) F-My1 peptide ITC binding isotherm titrated into PfMTIP. (g) Direct binding of F-My1 (red) and F-My2 (blue) to PfMTIP, measured by fluorescence anisotropy (n = 3).

(PV) membrane, and the parasite plasma membrane.[4] Previous research has elucidated the binding potential of a truncated MyoA peptide consisting of the C-terminal residues 799−816 with recombinant *Pf*MTIP. Although MyoA[799−816] is positively charged at physiological pH, suggesting some potential for uptake, the cell penetration properties have not previously been determined.[5,6] Another important consideration is the effect of parasite life stage on peptide uptake. The *Plasmodium* asexual cycle transitions through three developmental stages of growth over 48 h: rings, trophozoites, and schizonts. The ring stage initiates immediately postinvasion (PI) and is a relatively dormant phase; it is followed at ca. 12 h PI by the trophozoite stage, a period of intense growth for the parasite. An increased demand for nutrients during this rapid growth necessitates the formation of membrane channels, termed new permeability pathways (NPPs).[11] Peptides are known to be brought in *via* these NPPs, potentially providing a mechanism for delivery of a MyoA peptide.[12] Finally, at ca. 36 h PI, the parasite transitions to a schizont and transforms into many discrete merozoites, preparing for egress at 48 h PI and subsequent invasion of new host erythrocytes. *Pf*MTIP expression begins around 36 h PI peaking at around 42−45 h PI, with the MyoA:MTIP complex forming as early as 38 h PI.[13,14] We hypothesized that a high cellular concentration of truncated MyoA peptide delivered during the initiation of

https://dx.doi.org/10.1021/acschembio.0c00328
ACS Chem. Biol. 2020, 15, 1313−1320

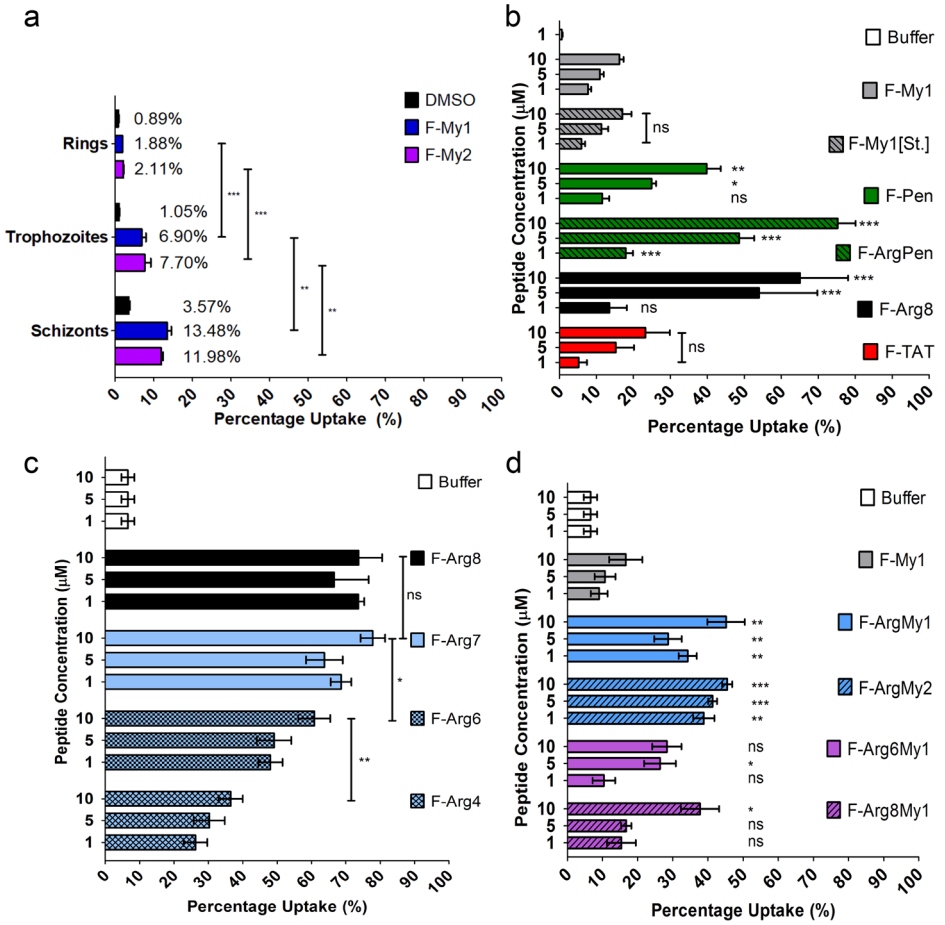

Figure 2. Cellular uptake of MyoA-derived peptides into *P. falciparum* analyzed by flow cytometry. (a) Uptake of F-My1 and F-My2 peptides over three stages of Pf3D7 lifecycle, percentage uptake calculated as number of FAM and DAPI positive cells (probe containing parasites) divided by all DAPI positive cells (total parasite population). Data generated by flow cytometry experiments; representative plots and gates plots are shown in Figure S6. Plasmodium cultures were incubated with peptides (1 μM) for 3 h. (b) Uptake of F-cell penetrating peptides (F-CPPs) into an early schizont culture of Pf3D7. Significance *t* test compares F-My1 to other peptides, at the same concentration. (c) Uptake of F-Arg$_n$ sequences into an early schizont culture of Pf3D7, demonstrating that chain length is important for peptide permeability. (d) Percentage uptake of modified MyoA peptide sequences, incorporating lessons learned from experiments with CPPs, into Pf3D7 early schizont cells. Significance *t* test compares F-My1 uptake with other peptides at the same concentration. For all plots, data represent mean ± SEM over six or more experimental replicates. *P* values compared using unpaired *t* test, buffer control vs peptide. ***p < 0.001, **p = 0.001−0.01, *p = 0.01−0.05, ns = nonsignificant.

MTIP expression could potentially disrupt the MyoA:MTIP PPI in schizonts.

MyoA[799−816], termed My1, is the minimal truncated MyoA peptide sequence necessary for tight binding with *Pf*MTIP *in vitro*, with a K_d = 73.8 ± 10.7 nM by isothermal titration calorimetry (ITC, Figure 1d, n = 2).[5,6,10] The observed binding affinity was concurrent with previously published values for the F-My1 peptide, K_d = 85 nM, also measured by ITC.[5] In order to enable detection and localization of the peptide within the *P. falciparum* parasite, an N-terminal 5(6)-carboxyfluorescein (FAM) moiety was added to the My1 peptide separated by a glycine spacer; this peptide was termed F-My1. A weaker-binding control was synthesized with a double mutation exchanging two residues from the hydrophilic and hydrophobic faces of the buried MTIP:MyoA interaction: F-My1 (R806A/A809R), termed F-My2 (sequences shown in Figure 1c).[6]

This approach was favored oversimple alanine mutation in order to keep the overall charge of both peptides the same and enable pairwise comparisons for parasite uptake. F-My1 and F-My2 were assayed by ITC and fluorescence anisotropy (FA). ITC showed that incorporation of N-terminal FAM was well tolerated in F-My1 (Figure 1d,f) with binding affinities remaining in the low nanomolar range (K_d = 57 ± 13 nM), comparable to that of MyoA[799−816] peptide (K_d = 85 ± 6 nM).[5] Affinities determined by FA were somewhat lower (Figure 1g) with F-My1 (K_d = 8.7 ± 0.6 nM), while F-My2 showed a 40-fold reduction in affinity for *Pf*MTIP (K_d = 394 ± 16 nM). A competitive inhibition assay format (Figure S1) confirmed that the corresponding unlabeled peptides My1 and My2 could outcompete F-My1 binding to *Pf*MTIP with IC_{50} values of 67 nM and 6880 nM, respectively.

With high-affinity and control (reduced-affinity) peptide probes in hand, parasite cell permeability was first investigated quantitatively using flow cytometry. Peptides (1 μM) were incubated with *P. falciparum* (3D7 strain) for 3 h during each of three *Plasmodium* life stages (ring, trophozoite, and schizont). Flow cytometry demonstrated that cell permeability of F-My1 and F-My2 was generally low and heavily dependent on the lifecycle stage (Figure 2a), peaking at 13 ± 1% for F-My1 in schizonts. A possible explanation for the increased uptake in late stage parasites is peptide entry through an NPP

https://dx.doi.org/10.1021/acschembio.0c00328
ACS Chem. Biol. 2020, 15, 1313−1320

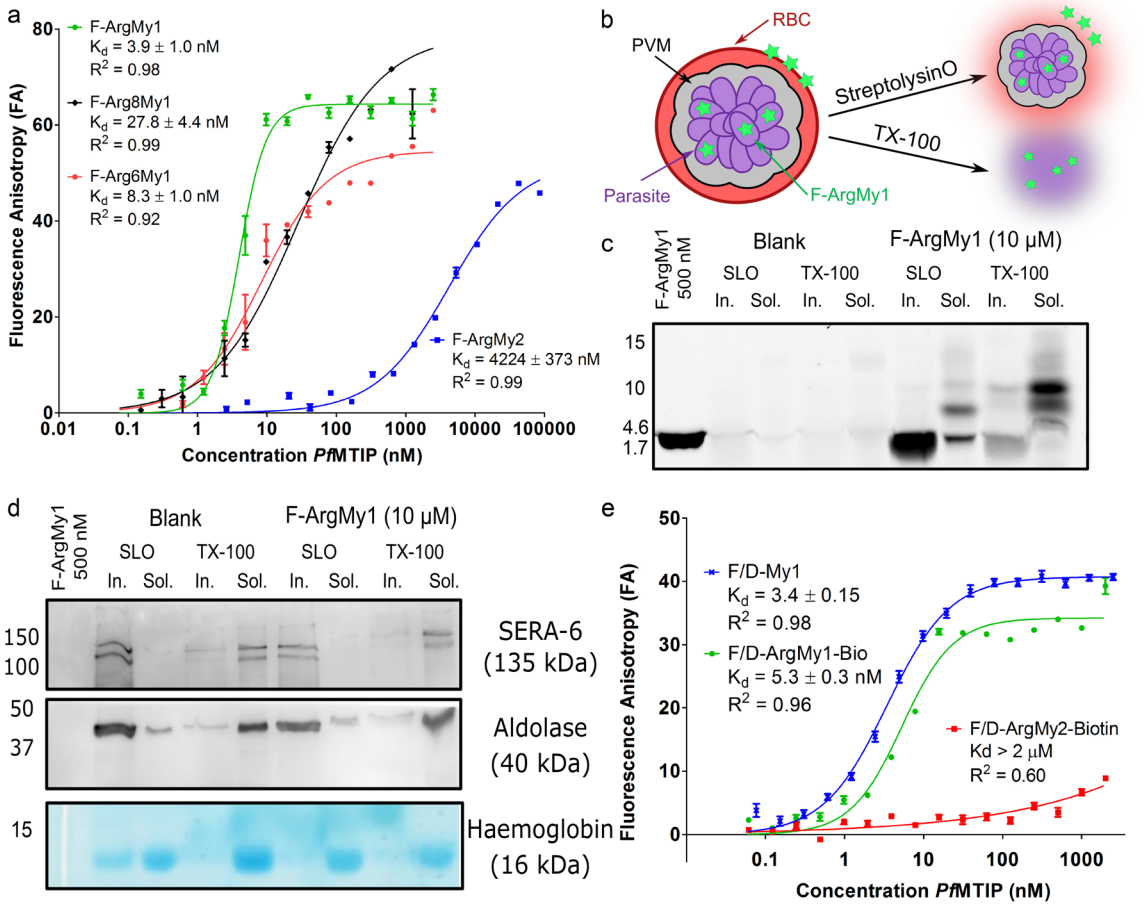

Figure 3. Cellular localization of peptide probe in *P. falciparum* measured by biochemical assays. (a) Fluorescence anisotropy binding assay data for modified MyoA-based peptides with improved uptake in Plasmodium3D7 cells, $n = 3$. (b) Schematic adapted from Ruecker *et al.* showing selective lysis of the three membranes (erythrocyte plasma, parasitophorous vacuole, and Plasmodiumplasma) with separate detergents, to determine if peptide probe penetrates the parasitized cell or adheres to the RBC membrane.[25] (c) IGF fluorescein signal, SDS-PAGE samples of insoluble and soluble lanes of both treatment, run on a high percentage gel (16%/6 M Urea TrisTricine).[26] (d) Western blot controls demonstrating selective lysis of membranes, SERA-6 (135 kDa, PVM protein) and PfAldolase (40 kDa parasite protein) are only released into soluble fraction after treatment with TX-100. Coomassie shows hemoglobin released into soluble fraction after treatment with SLO. (e) Fluorescence anisotropy binding assay data for diazirine and biotin containing MyoA-based peptides.

present only at late stages of schizogony. Alternatively, it may be due to increased leakiness of red blood cell and parasitophorous vacuole (PV) membranes when the cytoskeleton is broken down as the parasite prepares to egress.[15] Regardless, it was necessary to optimize the peptide sequence to improve its cell permeability properties to enable uptake in earlier life stages, before the formation of the *Pf*MyoA:MTIP complex.[13,14]

Modification to increase positive charge or by conjugation with one of the varied cell penetrating peptide (CPP) sequences found in nature is a widely explored approach to improve cellular permeability of peptides.[16−18] Despite the ubiquity of CPPs in this context there is a paucity of data regarding their uptake into *P. falciparum* cells, with the exception of polyarginines.[19] A panel of eight CPPs, TAT48−60, penetratin, arginine−penetratin, and various polyarginines, were synthesized, all bearing an N-terminal FAM moiety. A pentenyl alanine stapled version F-MyoA pAla[811,815], termed F-My1[St.],[20,21] was also synthesized based on previous evidence that stapling improved uptake of an unrelated peptide into *P. falciparum* as early as the trophozoite stage.[22] The uptake properties of these peptides were tested with *P. falciparum* early schizonts (ca. 35 h PI), which is the hypothesized window for target engagement prior to *Pf*MyoA:MTIP complex formation *in vivo*.[14] Uptake data (Figure 2b) showed no significant improvement with the addition of the staple, F-My1[St.], and TAT48−60 displayed similar uptake to F-My1. Three peptides showed significantly greater permeability over F-My1; these were penetratin (F-Pen), arginine−penetratin (F-ArgPen, a penetratin sequence where lysine residues were mutated to arginine), and octo-arginine (F-Arg8).[23] Further investigation showed that uptake into *P. falciparum* early schizonts correlates positively with the length of polyarginine peptide with F-Arg7 and F-Arg8 significantly greater than F-Arg6, which in turn shows a significant improvement over F-Arg4 (Figure 2c).[24] Three peptides were synthesized building on these results: two MyoA sequences with N-terminal octo/hexa-arginine (F-Arg8My1 and F-Arg6My1) and a MyoA mutant carrying strategically placed lysine to arginine mutations (F-ArgMy1), giving a total of five Arg residues within the peptide while retaining the distribution of positive charge across the helix. Encouragingly, F-ArgMy1 and F-Arg8My1 showed 2-fold improvement in uptake compared to F-My1 (Figure 2d). These sequence

https://dx.doi.org/10.1021/acschembio.0c00328
ACS Chem. Biol. 2020, 15, 1313−1320

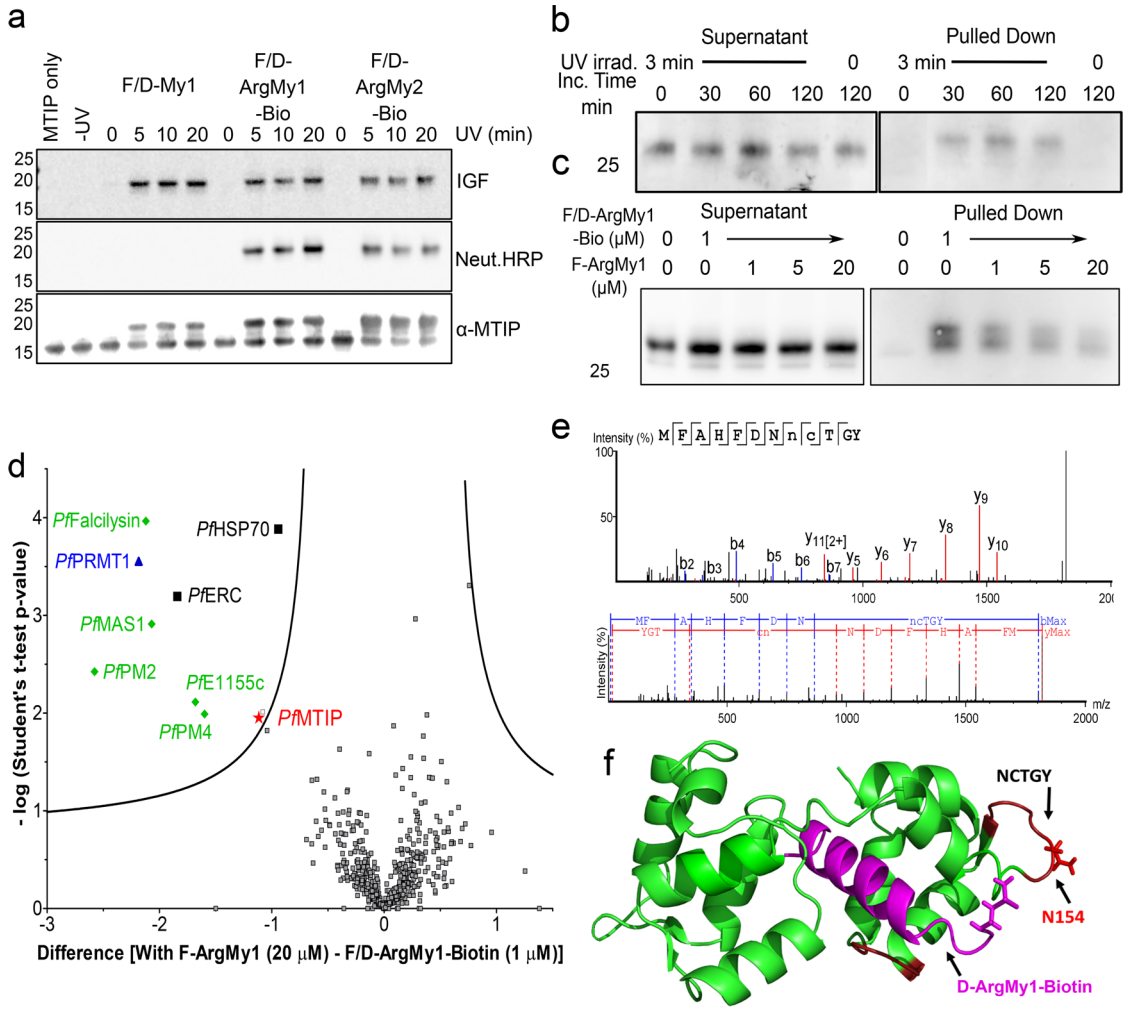

Figure 4. Selective engagement of modified F-ArgMy1 peptides with native target protein *Pf*MTIP. (a) IGF, α-neutravidin-HRP, and Rb α-MTIP Western blots showing MyoA based diazirine peptides (5 μM) can label *Pf*MTIP (1 μM). (b) α-MTIP WB showing successful pulldown of *Pf*MTIP from *Pf*3D7 schizont lysate. NB- D, 0 min incubation, run on separate SDS-PAGE, full gels shown in Supporting Information Figure 3. (c) α-MTIP WB, 90 μg of *Pf*3D7 late schizont lysate used in all conditions, incubated with F/D-ArgMy1-Bio (5 μM) and with increasing concentrations of F-ArgMy1 as an inhibitor; blot shows successful inhibition of *Pf*MTIP pulldown. (d) Proteomics data, statistical analysis by *t* test, FDR = 0.15, s0 = 0.4. Inhibition of enrichment of *Pf*MTIP (red) using F-ArgMy1 (20 μM). Nine significant hits that are significant both in blank vs F/D-ArgMy1-Bio experiment and in inhibition experiment are highlighted: *Pf*MTIP (red), peptidases (green), Arg-NMT transferase (blue), and high abundance proteins HSP70 and ERC (black). 60S ribosomal protein (gray) was observed as significant in the inhibition experiment only and so was discounted. Proteins with positive significant difference in inhibited triplicate (purple) were disregarded. (e) Resolved mass spectrum, showing modified *Pf*MTIP residue is Asn-154 (red), also shown. (f) Modified crystal structure (PDB 4AOM) of *Pf*MTIP (green) with MyoA[799−816], adapted to include N-terminal Gly-methionine to model site of modification with photomethionine (purple).

modifications were also well-tolerated, retaining low nanomolar binding affinities in the FA binding assay (Figure 3a). For reasons of similarity in molecular weight and sequence to F-My1, F-ArgMy1 was selected as the lead peptide probe for the following experiments.

We next explored distribution of F-ArgMy1 within the *P. falciparum* cell. In order to confirm that F-ArgMy1 was not simply adhering to the RBC membrane, an established procedure was adapted to selectively lyse the red blood cell (RBC) membrane, parasitophorous vacuole membrane (PVM), and *Plasmodium* plasma membrane.[25] A functional MyoA peptide probe would need to penetrate all three of these membranes to reach its PPI target. Aliquots of *P. falciparum* late schizonts were incubated with F-ArgMy1 (10 μM) and a buffer control for 3 h. Cells were then treated with either streptolysin-O (SLO) or 1% TX-100, in order to lyse either the RBC or all three membranes, respectively (Figure 3b).

The results were analyzed by SDS-PAGE gel electrophoresis, using 16%/6 M urea Tris-tricine gels suitable for resolution and retention of low molecular weight peptides, and by Western blot.[26] In-gel fluorescence was used to observe peptide localization *in vivo*; after SLO treatment (to lyse the RBC membrane) the vast majority of fluorescence signal was observed in the insoluble fraction (Figure 3c). However, upon treatment with TX-100 (to lyse the PV and parasite membranes), the peptide signal was observed in the soluble fraction, indicating that the peptide penetrates the parasitized erythrocyte rather than simply adhering to the RBC membrane. Interestingly, the peptide displays an increase in apparent molecular weight in parasite samples treated with TX-100. While this could be the result of *in vivo* modifications to the peptide, samples of F-ArgMy1 (500 nM) treated with a serial dilution of TX-100 also displayed an increase in apparent molecular weight, making it likely that this is an effect of the

https://dx.doi.org/10.1021/acschembio.0c00328
ACS Chem. Biol. 2020, 15, 1313−1320

detergent on migration in the highly cross-linked gel (Figure S7). The specificity of lysis was confirmed by Coomassie and Western blot (Figure 3d). Coomassie shows the release of hemoglobin from the erythrocyte cytoplasm upon treatment with SLO, while parasite proteins *Pf*SERA6 and *Pf*Aldolase (found in the PV and parasite cytoplasm respectively) remain in the insoluble fraction, indicating that the PV and parasite membranes remained intact. As expected, both proteins were released into the soluble fraction after treatment with TX-100.

An estimation of *in vivo* F-ArgMy1 concentration was made by densitometric analysis of IGF image (Figure 3c), performed using ImageQuant FL software. Calculations (eq S1 and Table S1) indicate that the concentration of F-ArgMy1 released into the soluble fraction by SLO and TX-100 treatments was 2.5 ± 0.5 and 5.1 ± 2.1 μM, respectively; this indicated that ca. 2.6 μM F-ArgMy1 was attained within the PV. While quantitative analyses from densitometric data should not be over-interpreted, they provide a useful indication of the likely order of magnitude of peptide uptake, and suggest that F-ArgMy1 released into the soluble fractions by SLO and TX-100 is in the low micromolar range. While this estimated concentration is above the K_d value for F-ArgMy1 binding with *Pf*MTIPΔ60, this experiment gave no indication of the *in vivo* state of the peptide, and whether it was still in a form which could bind with endogenous *Pf*MTIP or had been degraded. Taken together, data from cytometry and biochemical analysis support the conclusion that F-ArgMy1 is cell permeable, enters intact *P. falciparum* cells within infected RBCs, and may reach the correct cellular compartment at a concentration sufficient to engage its target.

To further validate the peptide as a potential probe *in vivo*, we sought to demonstrate engagement with endogenously expressed *Pf*MTIP, known to carry a number of PTMs which may affect the binding affinity with the ArgMy1 probe compared to recombinant *Pf*MTIPΔ60.[5] To facilitate target engagement experiments, a diazirine moiety was added to the N-terminus of F-My1 and F-ArgMy1 sequences in the form of a diazirine-bearing photomethionine residue (F/D-My1 and F/D-ArgMy1), alongside analogues bearing a C-terminal biotin for use in pull down and proteomics experiments.[27] These modifications were tolerated, with F/D-ArgMy1-biotin displaying low nanomolar binding affinity with *Pf*MTIP, K_d = 5.3 nM ± 0.3 nM (Figure 3e). A nonbinding control, termed F/D-ArgMy2-Biotin, was also synthesized bearing the same modifications at the N- and C-termini (Table S2). The binding affinity was reduced by the exchange of two pairs of amino acids from the hydrophobic and hydrophilic faces of the peptide K_d > 2 μM (Figure 3e). As a proof of concept for photo-cross-linking, recombinant *Pf*MTIPΔ60 (19 kDa, 1 μM) was incubated with F/D-My1 or F/D-ArgMy1 and 2-Biotin (5 μM) for 30 min and then irradiated with UV light (365 nm, 3 min). Successful cross-linking was demonstrated by in-gel fluorescence, with a fluorescein signal observable in bands with the expected product mass (21 kDa) in probe containing lanes (Figure 4a). α-MTIP WB validated that bands at 19 and 21 kDa were *Pf*MTIP, with and without cross-linking to a probe. Additionally, WB against neutravidin-HRP confirmed that the C-terminal biotin is accessible when F/D-ArgMy1 is cross-linked to the target protein. F/D-ArgMy1-biotin was next taken forward to experiments with *P. falciparum* lysate to test engagement with endogenously expressed *Pf*MTIP.

Endogenous *Pf*MTIP cross-linking experiments were performed by incubating F/D-ArgMy1-biotin with *P. falciparum* late schizont lysate, when *Pf*MTIP is expected to be maximally expressed.[13,14] Cross-linked lysate was precipitated and resolubilized, to remove excess probe, before being incubated with streptavidin-coated Dynabeads (C1) to enrich labeled proteins. Antibodies against *Pf*MTIP confirmed the presence of cross-linked-*Pf*MTIP bands (21 kDa) in a probe- and UV-dependent manner by immunoblot (Figure 4b). Competition experiments against a dilution series of F-ArgMy1 further demonstrated the specificity of cross-linking between F/D-ArgMy1-biotin and native *Pf*MTIP in schizont lysate (Figure 4c). Further validation of the interaction between F/D-ArgMy1-biotin and endogenous *Pf*MTIP was conducted by quantitative proteomic analysis using nanoLC-MS/MS. Triplicate samples of *P. falciparum* schizont lysate were treated with F/D-ArgMy1-Bio (1 μM), F/D-ArgMy1-Bio (1 μM) + F-ArgMy1 (20 μM) probe, and a DMSO control. The cells were lysed (1% TX-100 buffer) and processed using a pull-down and quantitative proteomics workflow detailed in the Methods section, and analyzed by mass spectrometry. Of 563 proteins identified, it was shown that 430, including *Pf*MTIP, were significantly enriched in a probe over DMSO conditions (Figure S4). Of these 430 proteins, only nine were both significant in the blank vs probe experiment and significantly outcompeted by F-ArgMy1 (20 μM; Figure 4d), with *Pf*MTIP (red) among these hits (Table S3). The remaining eight proteins are unrelated to the *Plasmodium* glideosome and are likely off-target hits driven by electrostatic interactions of an arginine rich peptide probe. The mean isoelectric points of peptides identified for each protein were all below seven (Table S4). These included five peptidases, an arginine *N*-methyltransferase, and two high-abundance proteins (endoplasmic reticulum calcium-binding protein and chaperone protein HSP70).

Finally, in order to observe if the modified peptide was binding in a plausible manner to *Pf*MTIP, cross-linked *Pf*MTIP tryptic peptides were searched by *de novo* sequencing, using PEAKS software.[28] In experiments with F/D-ArgMy1-Bio, no such fragments were observable, hypothesized to be due to the larger sized modification due to fluorescein and photomethionine flying poorly in the mass spectrometer. Therefore, the experiment was repeated using recombinant *Pf*MTIP and D-My1-Bio resulting in a smaller modification after trypsin digestion, and peptide fragment spectra that clearly show cross-linking to a specific *Pf*MTIP amino acid residue Asn154, bearing a photoMet-Gly modification (Figure 4e). All peptides bearing this addition were seen to originate from the C-terminal domain of *Pf*MTIP, indicating that the modified peptide was binding in the expected manner with *Pf*MTIP. A model of F/D-ArgMy1[799−816] bound to *Pf*MTIP (PDB 4AOM) highlights the diazirine modified regions in red (Figure 4f).[5] Despite multiple attempts, *in vivo* cross-linking experiments did not show any cross-linking between probe and parasite proteins. While there are a number of reasons this experiment could have failed, we hypothesize that the absorption of UV light by hemoglobin could stop the diazirine moiety from being activated properly.

Despite a dramatic improvement in the uptake properties of the MyoA-based peptide probe, efforts to replicate the cell viability phenotype claimed by Bosch et al. were unsuccessful (Figure S5a) with an observed EC_{50} ≈ 160 μM for each of F-My1, F-ArgMy1, and F-ArgMy3. These peptides have

https://dx.doi.org/10.1021/acschembio.0c00328
ACS Chem. Biol. 2020, 15, 1313−1320

drastically different binding affinities with *Pf*MTIP as well as differing uptake properties into *Plasmodium* cells, and this result suggests that the observed toxicity is not the result of a specific interaction with endogenous *Pf*MTIP.

Here, we have presented the development of a novel truncated MyoA-based peptide as a probe for a key PPI found in the invasion machinery of the malaria parasite *P. falciparum*. While initial flow cytometry experiments revealed the poor permeability of the MyoA[799−816] peptide, valuable insights were gained through permeability experiments using CPPs, some of which were tested for the first time here in *P. falciparum*. Targeted sequence modifications replacing three lysine residues with arginine resulted in probe F-ArgMy1, which showed significantly improved permeability in midstage schizonts, up to 50% of all parasitized cells. Furthermore, this peptide was shown to permeate the parasitized cell by biochemical experiments based on selective membrane lysis, reaching at least as far as the PV space at concentrations sufficient to detect directly by gel-based analysis, estimated to be 2.5 μM. Improved uptake was not to the detriment of affinity, as the peptide retained low nanomolar binding affinity. A photoaffinity probe, F/D-ArgMy1-Biotin, successfully demonstrated target engagement and enrichment of endogenously expressed *Pf*MTIP from schizont lysate, and pull-down competition experiments demonstrate selectivity of *Pf*MTIP enrichment by quantitative proteomics, along with the identification of several off-targets. The site of modification with this probe was also consistent with structural prediction of the peptide-MTIP complex, based on a cocrystal structure of MyoA[799−816] and MTIP.

These results demonstrate a step forward in the development of a truncated MyoA peptide as a tool to investigate the potential druggability of the MyoA:MTIP PPI, achieving delivery of intact peptide to live intracellular parasites as judged by biochemical and fluorescence analyses. However, to date, direct evidence for target engagement in intact parasites has not been achieved, and despite enhanced uptake and high affinity binding, optimized probes do not block parasite invasion in a manner consistent with inhibition of MyoA:MTIP complex formation. These results may imply that the peptide probe does not access the correct compartment (the inner membrane complex, IMC, Figure 1a) at a sufficient concentration or that MyoA:MTIP is formed very rapidly following biosynthesis and is then resistant to inhibition. Indeed, there is evidence that MyoA:MTIP is formed as an intact complex prior to transport to the IMC, which may complicate targeting of this interaction; MTIP is also modified by phosphorylation, which has been hypothesized to regulate its interaction with MyoA.[5,29,30] The MyoA:MTIP complex is part of a much larger assembly at the IMC, and it is also plausible that these interactions add to its stability. Future studies may consider whether peptides can disrupt the preformed complex; however, biochemical reconstitution of a full glideosome complex is challenging and has not been reported to date, making further *in vitro* assessment of this target interaction problematic. Finally, it may be the case that effective inhibition of MyoA:MTIP does not substantially impact invasion, which would invalidate this complex as an antimalarial target.

In conclusion, the work presented here provides new insights into the design of parasite-penetrant peptide probes, and the potential druggability of the MyoA:MTIP interaction. Our data suggest that this PPI is a highly challenging target, and that future work should focus on establishing evidence for engagement *in vivo* to provide evidence to validate or invalidation MyoA:MTIP inhibitors as potential antimalarial agents.

■ ASSOCIATED CONTENT

Supporting Information

The Supporting Information is available free of charge at https://pubs.acs.org/doi/10.1021/acschembio.0c00328.

Detailed experimental procedures, list of materials used, supplementary figures and tables (PDF)

■ AUTHOR INFORMATION

Corresponding Author

Edward W. Tate − *Department of Chemistry and Institute of Chemical Biology, Molecular Sciences Research Hub, London W12 0BZ, United Kingdom;* orcid.org/0000-0003-2213-5814; Email: e.tate@imperial.ac.uk

Authors

Charlie N. Saunders − *Department of Chemistry and Institute of Chemical Biology, Molecular Sciences Research Hub, London W12 0BZ, United Kingdom*

Ernesto Cota − *Department of Life Sciences, Imperial College, London SW7 2AZ, United Kingdom*

Jake Baum − *Department of Life Sciences, Imperial College, London SW7 2AZ, United Kingdom*

Complete contact information is available at: https://pubs.acs.org/10.1021/acschembio.0c00328

Notes

The authors declare no competing financial interest.

■ ACKNOWLEDGMENTS

Acknowledgment is given to J. Strivastava (Imperial College Flow, Lab Manager) for help with flow cytometry experiments; C. LingTay for training the author in *Plasmodium falciparum* cell culture methodologies; A. Barnard for the synthesis of Fmoc-Photomethionine; and A. Barnard and T. Laynon-Hogg for proof reading this manuscript. This work was supported by the Institute for Chemical Biology, EPSRC Centre for Doctoral Training (Imperial College London), EPSRC Grant EP/L015498/1, Reference 1508866. Parasite tissue culture work was supported by Wellcome (Investigator to J.B. 100993/Z/13/Z).

■ REFERENCES

(1) World Malaria Report 2017. *WHO Reports*; World Health Organzation, 2018; p 196.

(2) Powell, C. J., Ramaswamy, R., Kelsen, A., Hamelin, D. J., Warshaw, D. M., Bosch, J., Burke, J. E., Ward, G. E., and Boulanger, M. J. (2018) Structural and Mechanistic Insights into the Function of the Unconventional Class XIV Myosin MyoA from Toxoplasma Gondii. *Proc. Natl. Acad. Sci. U. S. A. 115* (45), E10548−E10555.

(3) Mbengue, A., Bhattacharjee, S., Pandharkar, T., Liu, H., Estiu, G., Stahelin, R. V., Rizk, S. S., Njimoh, D. L., Ryan, Y., Chotivanich, K., et al. (2015) A Molecular Mechanism of Artemisinin Resistance in Plasmodium Falciparum Malaria. *Nature 520* (7549), 683−687.

(4) Farrow, R. E., Green, J., Katsimitsoulia, Z., Taylor, W. R., Holder, A. A., and Molloy, J. E. (2011) The Mechanism of Erythrocyte Invasion by the Malarial Parasite, Plasmodium Falciparum. *Semin. Cell Dev. Biol. 22* (9), 953−960.

(5) Douse, C. H., Green, J. L., Salgado, P. S., Simpson, P. J., Thomas, J. C., Langsley, G., Holder, A. A., Tate, E. W., and Cota, E. (2012) Regulation of the Plasmodium Motor Complex: Phosphorylation of Myosin a Tail-Interacting Protein (MTIP) Loosens Its Grip on MyoA. *J. Biol. Chem. 287* (44), 36968−36977.
(6) Thomas, J. C., Green, J. L., Howson, R. I., Simpson, P., Moss, D. K., Martin, S. R., Holder, A. A., Cota, E., and Tate, E. W. (2010) Interaction and Dynamics of the Plasmodium Falciparum MTIP-MyoA Complex, a Key Component of the Invasion Motor in the Malaria Parasite. *Mol. BioSyst. 6* (3), 494−498.
(7) Baum, J., Papenfuss, A. T., Baum, B., Speed, T. P., and Cowman, A. F. (2006) Regulation of Apicomplexan Actin-Based Motility. *Nat. Rev. Microbiol. 4* (8), 621−628.
(8) Egarter, S., Andenmatten, N., Jackson, A. J., Whitelaw, J. A., Pall, G., Black, J. A., Ferguson, D. J. P., Tardieux, I., Mogilner, A., and Meissner, M. (2014) The Toxoplasma Acto-MyoA Motor Complex Is Important but Not Essential for Gliding Motility and Host Cell Invasion. *PLoS One 9* (3), No. e91819.
(9) Robert-Paganin, J., Robblee, J. P., Auguin, D., Blake, T. C. A., Bookwalter, C. S., Krementsova, E. B., Moussaoui, D., Previs, M. J., Jousset, G., Baum, J., et al. (2019) Plasmodium Myosin A Drives Parasite Invasion by an Atypical Force Generating Mechanism. *Nat. Commun. 10* (1), 3286.
(10) Bosch, J., Turley, S., Daly, T. M., Bogh, S. M., Villasmil, M. L., Roach, C., Zhou, N., Morrisey, J. M., Vaidya, A. B., Bergman, L. W., et al. (2006) Structure of the MTIP-MyoA Complex, a Key Component of the Malaria Parasite Invasion Motor. *Proc. Natl. Acad. Sci. U. S. A. 103* (13), 4852−4857.
(11) Ginsburg, H., and Stein, W. D. (2004) The New Permeability Pathways Induced by the Malaria Parasite in the Membrane of the Infected Erythrocyte: Comparison of Results Using Different Experimental Techniques. *J. Membr. Biol. 197* (2), 113−122.
(12) Saliba, K. J., and Kirk, K. (1998) Uptake of an Antiplasmodial Protease Inhibitor into Plasmodium Falciparum-Infected Human Erythrocytes via a Parasite-Induced Pathway. *Mol. Biochem. Parasitol. 94* (2), 297−301.
(13) Green, J. L., Martin, S. R., Fielden, J., Ksagoni, A., Grainger, M., Yim Lim, B. Y. S., Molloy, J. E., and Holder, A. A. (2006) The MTIP-Myosin A Complex in Blood Stage Malaria Parasites. *J. Mol. Biol. 355* (5), 933−941.
(14) Green, J. L., Wall, R. J., Vahokoski, J., Yusuf, N. A., Ridzuan, M. A. M., Stanway, R. R., Stock, J., Knuepfer, E., Brady, D., Martin, S. R., Howell, S. A., Pires, I. P., Moon, R. W., Molloy, J. E., Kursula, I., Tewari, R., Holder, A. A., et al. (2017) Compositional and Expression Analyses of the Glideosome during the Plasmodium Life Cycle Reveal an Additional Myosin Light Chain Required for Maximum Motility. *J. Biol. Chem. 292* (43), 17857−17875.
(15) Millholland, M. G., Chandramohanadas, R., Pizzarro, A., Wehr, A., Shi, H., Darling, C., Lim, C. T., and Greenbaum, D. C. (2011) The Malaria Parasite Progressively Dismantles the Host Erythrocyte Cytoskeleton for Efficient Egress. *Mol. Cell. Proteomics 10* (12), No. M111.010678.
(16) Kolesinska, B., Podwysocka, D. J., Rueping, M. A., Seebach, D., Kamena, F., Walde, P., Sauer, M., Windschiegl, B., Meyer-Ács, M., Vor Der Brüggen, M., et al. (2013) Permeation through Phospholipid Bilayers, Skin-Cell Penetration, Plasma Stability, and CD Spectra of α- And β-Oligoproline Derivatives. *Chem. Biodiversity 10* (1), 1−38.
(17) Kamena, F., Monnanda, B., Makou, D., Capone, S., Patora-Komisarska, K., and Seebach, D. (2011) On the Mechanism of Eukaryotic Cell Penetration by α- and β-Oligoarginines–Targeting Infected Erythrocytes. *Chem. Biodiversity 8* (1), 1−12.
(18) Milletti, F. (2012) Cell-Penetrating Peptides: Classes, Origin, and Current Landscape. *Drug Discovery Today 17* (15−16), 850−860.
(19) Sparr, C., Purkayastha, N., Kolesinska, B., Gengenbacher, M., Amulic, B., Matuschewski, K., Seebach, D., and Kamena, F. (2013) Improved Efficacy of Fosmidomycin against Plasmodium and Mycobacterium Species by Combination with the Cell-Penetrating Peptide Octaarginine. *Antimicrob. Agents Chemother. 57* (10), 4689−4698.
(20) Douse, C. H., Maas, S. J., Thomas, J. C., Garnett, J. A., Sun, Y., Cota, E., and Tate, E. W. (2014) Crystal Structures of Stapled and Hydrogen Bond Surrogate Peptides Targeting a Fully Buried Protein-Helix Interaction. *ACS Chem. Biol. 9* (10), 2204−2209.
(21) Chu, Q., Moellering, R. E., Hilinski, G. J., Kim, Y. W., Grossmann, T. N., Yeh, J. T.-H., and Verdine, G. L. (2015) Towards Understanding Cell Penetration by Stapled Peptides. *MedChemComm 6* (1), 111−119.
(22) Flaherty, B. R., Wang, Y., Trope, E. C., Ho, T. G., Muralidharan, V., Kennedy, E. J., and Peterson, D. S. (2015) The Stapled AKAP Disruptor Peptide STAD-2 Displays Antimalarial Activity through a PKA-Independent Mechanism. *PLoS One 10* (5), No. e0129239.
(23) Bahnsen, J. S., Franzyk, H., Sandberg-Schaal, A., and Nielsen, H. M. (2013) Antimicrobial and Cell-Penetrating Properties of Penetratin Analogs: Effect of Sequence and Secondary Structure. *Biochim. Biophys. Acta, Biomembr. 1828* (2), 223−232.
(24) Seebach, D., Namoto, K., Mahajan, Y. R., Bindschädler, P., Sustmann, R., Kirsch, M., Ryder, N. S., Weiss, M., Sauer, M., Roth, C., et al. (2004) Chemical and Biological Investigations of Beta-Oligoarginines. *Chem. Biodiversity 1* (1), 65−97.
(25) Ruecker, A., Shea, M., Hackett, F., Suarez, C., Hirst, E. M. A, Milutinovic, K., Withers-Martinez, C., and Blackman, M. J. (2012) Proteolytic Activation of the Essential Parasitophorous Vacuole Cysteine Protease SERA6 Accompanies Malaria Parasite Egress from Its Host Erythrocyte. *J. Biol. Chem. 287* (45), 37949−37963.
(26) Schägger, H. (2006) Tricine-SDS-PAGE. *Nat. Protoc. 1* (1), 16−22.
(27) Vila-Perellö, M., Pratt, M. R., Tulin, F., and Muir, T. W. (2007) Covalent Capture of Phospho-Dependent Protein Oligomerization by Site-Specific Incorporation of a Diazirine Photo-Cross-Linker. *J. Am. Chem. Soc. 129* (26), 8068−8069.
(28) Tran, N. H., Qiao, R., Xin, L., Chen, X., Liu, C., Zhang, X., Shan, B., Ghodsi, A., and Li, M. (2019) Deep Learning Enables de Novo Peptide Sequencing from Data-Independent-Acquisition Mass Spectrometry. *Nat. Methods 16* (1), 63−66.
(29) Agop-Nersesian, C., Naissant, B., Ben Rached, F., Rauch, M., Kretzschmar, A., Thiberge, S., Menard, R., Ferguson, D. J. P., Meissner, M., and Langsley, G. (2009) Rab11A-Controlled Assembly of the Inner Membrane Complex Is Required for Completion of Apicomplexan Cytokinesis. *PLoS Pathog. 5* (1), e1000270.
(30) Ridzuan, M. A. M., Moon, R. W., Knuepfer, E., Black, S., Holder, A. A., and Green, J. L. (2012) Subcellular Location, Phosphorylation and Assembly into the Motor Complex of GAP45 during Plasmodium Falciparum Schizont Development. *PLoS One 7* (3), No. e33845.

https://dx.doi.org/10.1021/acschembio.0c00328
ACS Chem. Biol. 2020, 15, 1313−1320